Characterizing the Locality of Diabatic States for Electronic Excitation Transfer By Decomposing the Diabatic Coupling†

Josh Vura-Weis,‖ Marshall D. Newton,‡ Michael R. Wasielewski,‖ and Joseph E. Subotnik*,§

Department of Chemistry and Argonne-Northwestern Solar Energy Research (ANSER) Center, Northwestern University, Evanston, Illinois 60208-3113, Brookhaven National Laboratory, Upton, New York 11973, and Department of Chemistry, University of Pennsylvania, Philadelphia, Pennsylvania 19104-6323

Received: May 25, 2010; Revised Manuscript Received: August 28, 2010

A common strategy to calculate electronic coupling matrix elements for charge or energy transfer is to take the adiabatic states generated by electronic structure computations and rotate them to form localized diabatic states. In this paper, we show that, for intermolecular transfer of singlet electronic excitation, usually we cannot fully localize the electronic excitations in this way. Instead, we calculate putative initial and final states with small excitation tails caused by weak interactions with high energy excited states in the electronic manifold. These tails do not lead to substantial changes in the total diabatic coupling between states, but they do lead to a different partitioning of the total coupling between Coulomb (Förster), exchange (Dexter), and one-electron components. The tails may be reduced by using a multistate diabatic model or eliminated entirely by truncation (denoted as "chopping"). Without more information, we are unable to conclude with certainty whether the observed diabatic tails are a physical reality or a computational artifact. This research suggests that decomposition of the diabatic coupling between chromophores into Coulomb, exchange, and one-electron components may depend strongly on the number of states considered, and such results should be treated with caution.

1. Introduction

In order to model the flow of charge and energy in molecules and materials, one unavoidable question is: what are the initial and final states of electron and electronic excitation transfer (ET/EET) processes? These so-called "diabatic" states and their diabatic couplings are necessary inputs when calculating transfer rates within a golden rule (e.g., Marcus or Förster theory) framework. As such, there is a strong need for suitable models and robust algorithms to calculate them, and in recent years, a plethora of techniques have emerged for doing so. For a review of current techniques, see refs 1−5.

In this paper, our goal is to characterize the degree of localization of the diabatic states appropriate for singlet electronic excitation transfer (EET) processes when the donor and acceptor are well separated in space. In particular, we will ask a simple question: how localized is the excitation density in our representation of the initial and final states? And if there is delocalization, what is the physical meaning of such an effect? To answer these questions, we will initially study a small model system undergoing EET, the HeH^+ dimer, which can be treated both computationally and analytically. We will generate diabatic states using a new set of recently introduced transformations,[5,6] which can be classified as "localized diabatization" algorithms. The HeH^+ dimer presents no numerical complications due to the presence of bridges or (for sufficiently large donor/acceptor [D/A] separation) orbital mixing between D and A sites. As such, we can focus directly on the effects of through-space coupling between very well isolated monomers. The model calculations will then be supplemented by calculations and analysis of a more representative EET system, the perylenemonoimide−perylenediimide (PMI−PDI) dimer.

Two tools will be used to characterize the ultimate extent of localization of diabatic states. First, we will use a brute force approach of analyzing the components of the wave function one excitation at a time. Second, we will decompose the overall diabatic coupling into Coulomb, exchange, and one-electron contributions. This decomposition is common in the photochemistry literature for transfer of localized excitations,[7−9] where Coulomb coupling (often termed Förster-type[10−12]) is frequently described as "through space" and exchange coupling (Dexter-type[13]), often labeled "through bond", involves direct overlap between D and A. (Additional "1-electron" or "overlap" coupling terms are also discussed below.) For chromophores separated by distance X, the Coulomb component should decay as X^{-3}, while the exchange and one-electron terms should decay as $e^{-\beta X}$. Deviations from these idealized conditions indicate that the EET diabatic states are not behaving according to standard models[14] and may suggest the existence of diabatic tails. Note that in a Fermi's golden rule formalism, the rate of energy transfer is proportional to the square of the electronic coupling, such that the X^{-3} scaling of the Coulomb coupling will give the familiar X^{-6} scaling of the Förster rate.

The computational approach in this paper for constructing diabatic states, based on the variational electronic states of the entire excited DA supermolecule, is consistent with previous perturbational and variational supermolecule treatments.[15−18] Reference 18 includes comparisons with perturbational approaches based on isolated D and A species. Reference 17 provides an estimate of the range of X (<100 Å) for which the conventional picture based on coherent EET is valid, in contrast to very large X, where the mechanism involves uncorrelated absorption and emission events. The present focus on the role

† Part of the "Mark A. Ratner Festschrift".

* To whom correspondence should be addressed. E-mail: subotnik@sas.upenn.edu.

‖ Northwestern University.

‡ Brookhaven National Laboratory.

§ University of Pennsylvania.

10.1021/jp104783r
Published on Web 10/19/2010

of tails in long-range intermolecular EET is in contrast to previous work involving ET and EET in donor−bridge−acceptor (DBA) systems, in which the emphasis was on D and A tails penetrating into the bridge.[19,20]

The outline of this paper is as follows. In section 2, we will give a brief review of diabatization methods currently applied in computational chemistry and summarize localized diabatization for the reader. In section 3, we will address the question of the tails of diabatic states for EET, and show how such tails may be quantified by decomposing the total diabatic coupling. Numerical results are given for the model system (HeH^+ dimer) as well as the PMI-PDI dimer in section 4, and an analytical interpretation of our results is given in section 5. We discuss these results and conclude in section 6. Some specialized issues are discussed in the Appendix.

2. Brief Review of Diabatization Methods

2.1. Traditional Approaches. Before describing in detail our theoretical work based on localized diabatization, we remind the reader that, for a general ET or EET system, there can be no unique definition for constructing diabatic states. After all, the initial state of the system should depend on the initial state preparation. Moreover, if the event occurs in a condensed environment, we must accept our own lack of information about position and orientation of solvent molecules. For this reason, many chemical theorists have preferred in the past to avoid calculating diabatic states altogether, choosing instead to extract the electronic couplings necessary for predicting electron transfer rates using indirect methods.[21−28]

Notwithstanding this nonuniqueness, there are several different viable approaches for constructing diabatic states, which one can consider as alternatives to the "localized diabatization" we have implemented here. First, one can seek "historical" diabatic states for which the derivative couplings are equal to zero ($\langle \Phi_I(r; R)|\nabla_R|\Phi_J(r; R)\rangle_r = 0$).[29−31] Here, $|\Phi_I(r; R)\rangle$ and $|\Phi_J(r; R)\rangle$ are eigenvectors of the electronic Hamiltonian and $<...>_r$ signifies integration over all electronic degrees of freedom. As usual, r represents electronic coordinates and R represents nuclear coordinates.

Although this definition does not have any direct connection to ET or EET specifically, one can rationalize this definition by considering the full rovibronic Schrodinger equation: if adiabatic states diagonalize the electronic Hamiltonian, then it is plausible that diabatic states should be required to diagonalize the nuclear momentum operator. Unfortunately, however, such diabatic states are usually over determined and cannot be constructed exactly because of the large number of gradient components.[32] As such, only approximate solutions are possible.[31,33,34]

Besides the historical definition, a second approach is to construct diabatic states according to intuitively desirable physical or mathematical characteristics. On the one hand, the block diagonalization method by Koppel, Cederbaum, and Domcke[35−38] generates diabatic states by projecting a set of adiabatic states onto a reference set of target states. On the other hand, the Atchity-Ruedenberg scheme[39,40] searches for diabatic states with "configurational uniformity" over the entire potential energy surface; this scheme was later extended by the "fourfold way" of Nakamura and Truhlar,[41−43] who introduced the notion of "molecular orbital uniformity". Intuitively, all three of these approaches aim to minimize the derivative couplings implicitly by designing diabatic states whose potential energy surfaces do not have avoided crossings, where the derivative couplings can be exceedingly large.

In the specific context of ET/EET processes, a third approach to diabatization ignores derivative couplings entirely, and instead seeks diabatic states on the basis of other intuitive physical criteria. Examples of these methods in the context of electron transfer include generalized Mulliken Hush (GMH),[44,45] constrained DFT,[46−49] fragment charge difference (FCD),[50] and in the context of energy transfer, fragment energy difference (FED).[51−53] Recently, we added two new "localized diabatization" algorithms to this list of methods, namely Boys localization[6] (which is a generalization of GMH) and Edmiston−Ruedenberg (ER) localization.[5] These algorithms are closely tied to orbital localization from quantum chemistry.[54−60] The ER algorithm has the properties that (i) it applies to both electron and energy transfer; (ii) it applies to both inter- and intramolecular proceses and gives a balanced treatment of initial and final states; (iii) it is computationally feasible for large molecules with arbitrarily many charge or energy excitation centers; (iv) it treats molecules with arbitrary amounts of electron−electron correlation; (v) it relies on no fragment definitions; and (vi) it allows for the calculation of diabatic states at all nuclear geometries of the system. The GMH algorithm satisfies all of these criteria except (i) and (iii), whereas the Boys algorithm is limited to ET. For the latter reason, in the context of energy transfer, one must replace the Boys algorithm with an occupied-virtual separated "BoysOV" version,[61] as discussed below. Both the BoysOV and ER algorithms will be used in this paper.

2.2. Localized Diabatization. BoysOV and ER diabatization can be described with only a few elementary equations. By definition, for any problem in quantum mechanics, the adiabatic states of a system $|\Phi_j\rangle$ are those electronic states that diagonalize the electronic Hamiltonian. These electronic states are stationary assuming the system is closed and the nuclei remain fixed

$$H(r, R) = H_{\text{nuc}}(R) + H_{\text{el}}(r;R) \tag{1}$$

$$H_{\text{el}}(r;R)|\Phi_J(r;R)\rangle = E_J(R)|\Phi_J(r;R)\rangle \tag{2}$$

As before, r represents electronic coordinates and R represents nuclear coordinates. Capital Roman letters denote many-body electronic states, and when used below, lower case Roman letters will denote single electronic orbitals.

In contrast to stationary (adiabatic) states, the initial and final diabatic states in an ET or EET process are nonstationary with respect to H_{el}. One standard approach to describe these nonstationary states is to rotate the adiabatic states into a set of diabatic states $\{|\Xi_I\rangle\}$

$$|\Xi_I\rangle = \sum_{J=1}^{N_{states}} |\Phi_J\rangle U_{JI} \quad I = 1, ..., N_{\text{states}} \tag{3}$$

In typical intermolecular EET applications, where there is one acceptor species and one donor species, $N_{\text{states}} = 2$. For multichromophore complexes, however, one must set $N_{\text{states}} > 2$. For many calculations in this paper, we will use the 2-state model; however, crucial insights will be obtained from comparison with calculations for which more than two adiabatic states are mixed together.

The Boys and ER algorithms can be derived[5,6] by appealing to different models for system−solvent interactions that all lead to localization of some kind:

• Boys diabatization can be viewed in terms of a bath that exerts a constant electric field

• ER diabatization can be understood in terms of a bath exerting an electrostatic potential that responds linearly to the field of the system.

As a practical matter, the assumptions above lead to rotation matrices **U** characterized by maximizing two different localizing functions:

$$f_{\text{Boys}}(\mathbf{U}) = f_{\text{Boys}}(\{\Xi_I\}) = \sum_{I,J=1}^{N_{\text{states}}} |\langle \Xi_I|\vec{\mu}|\Xi_I\rangle - \langle \Xi_J|\vec{\mu}|\Xi_J\rangle|^2 \tag{4}$$

$$f_{\text{ER}}(\mathbf{U}) = f_{\text{ER}}(\{\Xi_I\}) = \sum_{I=1}^{N_{\text{states}}} \int d\tilde{\mathbf{r}}_1 \int d\tilde{\mathbf{r}}_2 \frac{\langle \Xi_I|\hat{\rho}(\tilde{\mathbf{r}}_2)|\Xi_I\rangle\langle \Xi_I|\hat{\rho}(\tilde{\mathbf{r}}_1)|\Xi_I\rangle}{|\tilde{\mathbf{r}}_1 - \tilde{\mathbf{r}}_2|} \tag{5}$$

where the density operator at position $\tilde{\mathbf{r}}$ is defined to be $\hat{\rho}(\tilde{\mathbf{r}})$:

$$\hat{\rho}(\tilde{\mathbf{r}}) = \sum_{j=1}^{\text{All Electrons}} \delta(\tilde{\mathbf{r}} - \hat{r}_{(j)}) \tag{6}$$

and $\hat{r}_{(j)}$ is the position operator for the jth electron.

From eq 4, we find that Boys localization is applicable only to charge separation. For energy transfer, we recently introduced an occupied-virtual separated BoysOV algorithm. This algorithm is only applicable to adiabatic states generated at the level of configuration interaction singles (CIS). In this case, one separates the dipole matrix into occupied-occupied and virtual−virtual components, and one maximizes the localization of the electron and hole separately

$$f_{\text{BoysOV}}(\mathbf{U}) = f_{\text{BoysOV}}(\{\Xi_I\}) = \sum_{I,J=1}^{N_{\text{states}}} |\langle \Xi_I|\vec{\mu}^{\text{occ}}|\Xi_I\rangle - \langle \Xi_J|\vec{\mu}^{\text{occ}}|\Xi_J\rangle|^2 + |\langle \Xi_I|\vec{\mu}^{\text{virt}}|\Xi_I\rangle - \langle \Xi_J|\vec{\mu}^{\text{virt}}|\Xi_J\rangle|^2 \tag{7}$$

where μ^{occ} and μ^{virt} are expressed in terms of second quantization. For more details, see ref 61.

2.3. The Case of More than Two Adiabatic States. Before concluding this discussion on localized diabatization, we must address the question of multiple diabatic states. In the case that we have multiple diabatic states with electronic excitation localized on the same monomer, we have found that it is crucial to rediagonalize the Hamiltonian within each monomer subspace. Doing so allows one to keep the monomer energies relatively constant. Moreover, from a physical perspective, this diagonalization accounts for the local relaxation that should occur quickly on each monomer subsequent to excitation.

3. Tails of Diabatic States

Our goal in this paper is to characterize the tails of diabatic states for singlet EET processes. Consider the intermolecular transfer of electronic excitation from donor D to acceptor A. If an asterisk represents an excited state, we expect that, to zeroth order, the initial and final states will be

$$|\Xi_I\rangle \stackrel{?}{=} |\text{D*A}\rangle \tag{8}$$

$$|\Xi_F\rangle \stackrel{?}{=} |\text{DA*}\rangle \tag{9}$$

We want to investigate, however, whether this is really so, if we use the localized diabatization routines discussed above. In particular, we wonder whether there might be tails such that

$$|\Xi_I\rangle \stackrel{?}{=} \alpha|\text{D*A}\rangle + \varepsilon|\text{DA*}\rangle \tag{10}$$

$$|\Xi_F\rangle \stackrel{?}{=} -\varepsilon|\text{D*A}\rangle + \alpha|\text{DA*}\rangle \tag{11}$$

where $\alpha^2 + \varepsilon^2 = 1$ and $\alpha \gg \varepsilon$. And, if these tails exist, what do they mean?

To that end, we will use CIS theory to generate the adiabatic states for an intermolecular dimer undergoing EET, and we will then perform either BoysOV and ER diabatization. In general these two methods give nearly identical results for all nonvanishing matrix elements. However, because we will deal with vanishingly small matrix elements in our study below of large donor−acceptor separations, with certain quantities only a few orders of magnitude larger than "machine epsilon" (i.e., couplings $\sim 10^{-8}-10^{-10}$ eV), we will report only results from BoysOV calculations. While the ER results are very similar, there is a larger source of numerical error when using two-electron integrals, and the BoysOV algorithm is slightly better behaved at very long distances.

Henceforward, the letters *ijkl* denote occupied orbitals and *abcd* denote virtual orbitals. Noting that CIS is invariant to orbital rotations, we will find it most convenient to use localized orbitals for the analysis in this paper. To that end, when computing the BoysOV localized diabatic states, we will analyze the results with Boys localized orbitals.[54−57] When treating donor−acceptor pairs at long distances, we will show that all orbitals (occupied and virtual) are strictly localized up to machine noise either on the left (donor) or the acceptor (right). In other words, at long distance, the tails of orbitals from monomer to monomer have amplitudes as small as can be expected from a finite precision machine. See Figure 4 and eqs 24 and 25.

We will restrict ourselves to closed shell singlet ground states, and the excited states will be labeled with capital letters *P*, *Q*, ... For singlet excited states, CIS adiabatic states are of the form

$$|\Phi_P\rangle = \sum_{ia} \frac{\tilde{t}_i^{Pa}}{\sqrt{2}}(c_a^\dagger c_i + c_{\bar{a}}^\dagger c_{\bar{i}})|\Phi_{\text{HF}}\rangle \tag{12}$$

$$= \sum_{ia} \frac{\tilde{t}_i^{Pa}}{\sqrt{2}}(c_a^\dagger c_i + c_{\bar{a}}^\dagger c_{\bar{i}})|\Phi_{\text{HF}}\rangle \tag{13}$$

$$= \sum_{ia} \frac{\tilde{t}_i^{Pa}}{\sqrt{2}}(|\Phi_i^a\rangle + |\Phi_{\bar{i}}^{\bar{a}}\rangle) \tag{14}$$

and diabatic states of the form

$$|\Xi_P\rangle = \sum_Q |\Phi_Q\rangle U_{QP} \qquad \mathbf{U}\mathbf{U}^{\mathrm{T}} = \mathbf{I} \tag{15}$$

$$= \sum_{ia} \frac{t_i^{Pa}}{\sqrt{2}} (c_a^\dagger c_i + c_{\bar{a}}^\dagger c_{\bar{i}}) |\Phi_{\mathrm{HF}}\rangle \tag{16}$$

$$= \sum_{ia} \frac{t_i^{Pa}}{\sqrt{2}} (|\Phi_i^a\rangle + |\Phi_{\bar{i}}^{\bar{a}}\rangle) \tag{17}$$

Note that, by our convention, the *t*-amplitude matrix has a tilde (~) in the adiabatic representation, but there is no tilde in the diabatic representation. Also, in the single-determinant states (Φ) and operators $c^\dagger$ and c in eqs 12−17, *ia* denote alpha spin orbitals, and $\bar{i}\,\bar{a}$ denote beta spin orbitals.

$$t_i^{Pa} = \sum_Q \tilde{t}_i^{Qa} U_{QP} \tag{18}$$

3.1. Diabatic Coupling. One means to study the tails of diabatic states is to sandwich the Hamiltonian between CIS diabatic wave functions and decompose the resulting diabatic couplings as follows:[62]

$$\left\langle \Phi_i^a | H | \Phi_j^b \right\rangle = E_0 \delta_{ij} \delta_{ab} + F_{ab} \delta_{ij} - F_{ij} \delta_{ab} + (ia|jb) - (ij|ab) \tag{19}$$

$$\langle \Xi_P | H | \Xi_Q \rangle = \underbrace{\sum_{iab} t_i^{Pa} t_i^{Qb} F_{ab} - \sum_{ija} t_i^{Pa} t_j^{Qa} F_{ij}}_{O} + \underbrace{2 \sum_{ijab} t_i^{Pa} t_j^{Qb} (ia|jb)}_{2J} - \underbrace{\sum_{ijab} t_i^{Pa} t_j^{Qb} (ij|ab)}_{K} \tag{20}$$

Here, **F** is the ground state Fock matrix and we are using chemists' notation for the two-electron integrals, e.g., (*ia*|*jb*). Note that eq 19 is written in terms of spin orbitals, and eq 20 is written in terms of spatial orbitals. O, 2J, and K correspond, respectively, to 1-electron (based on effective 1-electron Fock matrix elements), Coulomb, and exchange contributions to the total coupling.

The above decomposition is based on CIS supermolecule states expressed in terms of orthonormal MOs, and thus differs from analogous decompositions presented by Hsu et al[51,63] and by Scholes et al.[15,16,64] According to the Hsu/Scholes approaches, the coupling of nonorthogonal DA states was obtained, either from calculations of isolated D and A species[51,63] or from valence bond calculations with nonorthogonal local orbitals,[15,16,64] combined with perturbation theory. The 1-electron term O in eq 20 is analogous to (but quite distinct from) the "overlap" terms obtained from these nonorthogonal treatments[15,16,63,64] (e.g., the "penetration" term, P, in refs 15 and 16 is the analogue of the present O). A more detailed comparison of eq 20 and the expression given by Hsu et al. is given in the Appendix.

The decomposition in eq 20 gives us a window into the degree of localization of energetic excitations. Note that the individual *O*, *J*, and *K* terms are all completely well-defined tensor dot products, and do not depend on our choice of molecular orbitals. (The relative signs of H, O, J, and K are independent of the phases of the t^P and t^Q vectors, but the absolute signs do depend on these phases.) If we now assume that the orbital pairs *ia* and *jb* can be fully localized on separate D or A sites (i.e., $i \neq j$ and $a \neq b$), the *J* and *K* terms in eq 20 must correspond exactly to the Coulomb and exchange coupling discussed in traditional Förster and Dexter theory and *O* is zero. Moreover, in this case, we should expect that the *K* term will decrease exponentially with distance (i.e., $e^{-\beta X}$), while the *J* term will decrease asymptotically as X^{-3}. In the general CIS case, when the *O* term is not zero, *O* should decay exponentially as the monomers separate, because orbital localization is not absolute and scales exponentially with distance.

If the *O*, *J*, and *K* terms do not obey the rules listed above, we must conclude that our chemical intuition is failing, and that the diabatic states have unexpected features. We will find below that an abnormal decay of the *O*, *J*, and *K* terms can be explained by the existence of delocalized tails of electronic excitations.

3.2. Wave Function Analysis. Besides partitioning the Hamiltonian matrix elements, a second means to measure the size of the diabatic tails is to compute the norm of the t_i^a excitation vector on the different monomers. For instance, if $|\Xi_L\rangle$ is a diabatic state with the excitation energy primarily on the left, we can quantify how much excitation is on the right through the function ζ_{tail}

$$\zeta_{\mathrm{tail}}(\Xi_L) = \sum_{ia \in R} (t_i^a)^2 \tag{21}$$

The function ζ_{tail} should be rigorously zero if the entire electronic excitation is truly localized on one monomer or the other. Note that, for the molecular examples below, we have confirmed that the two lowest excited states have negligible charge transfer for $X \geq 5$ Å, i.e.

$$\sum_{i \in R\, a \in L} (t_i^a)^2 + \sum_{i \in L\, a \in R} (t_i^a)^2 \approx 0 \tag{22}$$

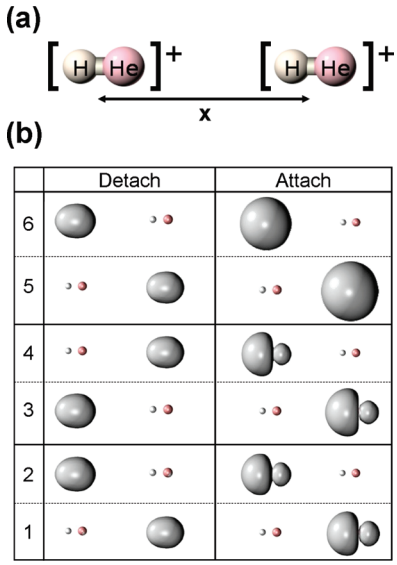

Figure 1. (a) Geometry used for our model calculations. The $(HeH)^+$ monomers are both aligned in the x direction and separated by a distance X in the x direction from midpoint to midpoint. The H−He distance is 1 Å. (b) Attachment-detachment plots for the first six adiabatic excited states for X = 6 Å.

Finally, the analysis above relies on our ability to localize orbitals either on the left or on the right monomer. If localized molecular orbitals are defined by

$$|i\rangle = \sum_{\mu} C_{\mu i}|\mu\rangle \quad |a\rangle = \sum_{\mu} C_{\mu a}|\mu\rangle \tag{23}$$

where atomic orbitals are indexed with the Greek letter μ, then the departure from orbital localization can be quantified according to

$$\chi_{\text{tail}}^{\text{occ}} = \sum_{i\in L\,\mu\in R} (C_{\mu i})^2 \tag{24}$$

$$\chi_{\text{tail}}^{\text{virt}} = \sum_{a\in L\,\mu\in R} (C_{\mu a})^2 \tag{25}$$

4. Numerical Results

4.1. Aligned HeH^+ Dimer. As our first numerical example, consider a dimer of aligned $(HeH)^+$ monomers separated at a distance X. See Figure 1a. For this molecular configuration, we have calculated the ground-state energy with HF and the singlet excited state energies with CIS. All calculations in this work were performed in the cc-pVDZ basis set using a locally modified version of Q-Chem.[65] The results are plotted in Figure 2. Note that in the chosen $C_{\infty v}$ geometry, the two monomers are not symmetry equivalent. The gap is nearly 20 eV between the ground state (S_0) and the first excited state (S_1). Between S_2 and S_3 there is asymptotically a gap of around 5 eV, and between S_4 and S_5 there is a gap of about 8 eV. The excited states come in nearly degenerate pairs, i.e., (S_1, S_2), (S_3, S_4), and (S_5, S_6). At distances longer than 2−3 Å, these pairs are usually separated only by tenths of an eV.

The character of the excited states is as follows:

• (S_1, S_2) are localized excitations. They are predominantly linear combinations of $HOMO_L \rightarrow LUMO_L$ and $HOMO_R \rightarrow LUMO_R$.

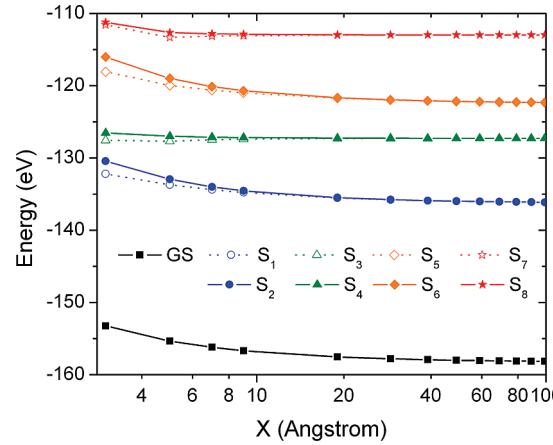

Figure 2. Adiabatic energies of $(HeH^+)_2$. The ground state is generated by Hartree−Fock and the excited states by CIS.

• (S_3, S_4) are charge transfer excitations. They are predominantly linear combinations of $HOMO_L \rightarrow LUMO_R$ and $HOMO_R \rightarrow LUMO_L$.

• (S_5, S_6) are localized excitations. They are predominantly linear combinations of $HOMO_L \rightarrow (LUMO + 1)_L$ and $HOMO_R \rightarrow (LUMO + 1)_R$.

Attachment detachment plots[66] for states S_1−S_6 are shown in Figure 1b.

4.2. 2-State Calculation. After calculating the adiabatic energies of the dimer in Figure 2, we applied BoysOV localization to generate a set of diabatic states for characterizing an EET event. In this case, naively, we expected to find two diabatic states, $|L^*R\rangle$ and $|LR^*\rangle$, where the electronic excitation is strictly localized either on the left (L) or on the right (R). Because the first and second excited states are so far removed from the next excited state, the simplest approach was to apply localized diabatization only to S_1 and S_2 (i.e., a 2-state model). Our results for the diabatic couplings in eq 20, i.e. the Coulomb J, exchange K and one-electron O matrix elements, are shown in Figure 3 (labeled 2-state results).

One conclusion from Figure 3 is that, for the 2-state model, where we include only the S_1 and S_2 states, the exchange and 1-electron terms are not zero even at 99 Å! In fact, they scale with distance as X^{-3}, which we expect only from the J term. These results are strong evidence that our diabatic states are not of the simple form $|L^*R\rangle$ and $|LR^*\rangle$. This interpretation is proven definitively in Figure 4 where we plot the function ζ_{tail} from eq 21. Here, we find that, if we construct diabatic states from only S_1 and S_2, then for a diabatic state with nearly all excitation on the left-hand monomer, there is always a tail of electronic excitation on the right-hand monomer up to very long distances. We also show (Figure 4) that the 1-electron localized orbitals are truly localized up to numerical noise by the time we reach X = 9 Å. Beyond this distance, any detected delocalization must be the result of applying localized diabatization to the CIS excited states.

4.3. Chopping Off the Tail. Although the 2-state model yields diabatic wave functions with tails, there are ways to generate diabatic states without tails. The crudest approach is to "chop off" these tails

$$|\Xi_I\rangle = \alpha|D^*A\rangle + \varepsilon|DA^*\rangle \xrightarrow{\text{chop}} |\Xi_I^c\rangle = \alpha|D^*A\rangle \tag{26}$$

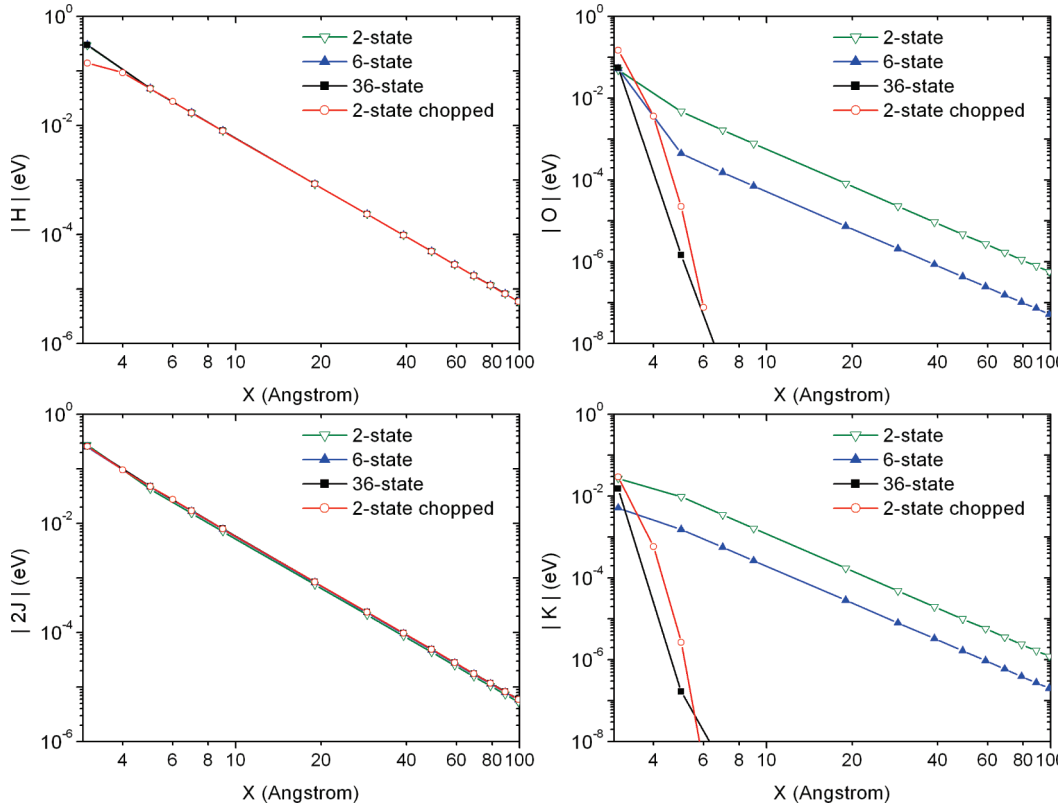

Figure 3. Matrix elements J, K, and O that make up the total diabatic coupling H. If electronic excitation were completely localized on one monomer or the other, the O and K terms should decay exponentially. Here, we plot the absolute value of each matrix element using both the 2-state model, and models where we either include more excited states or simply chop off the delocalized tails. For H and J, the four lines plotted nearly overlap on this scale.

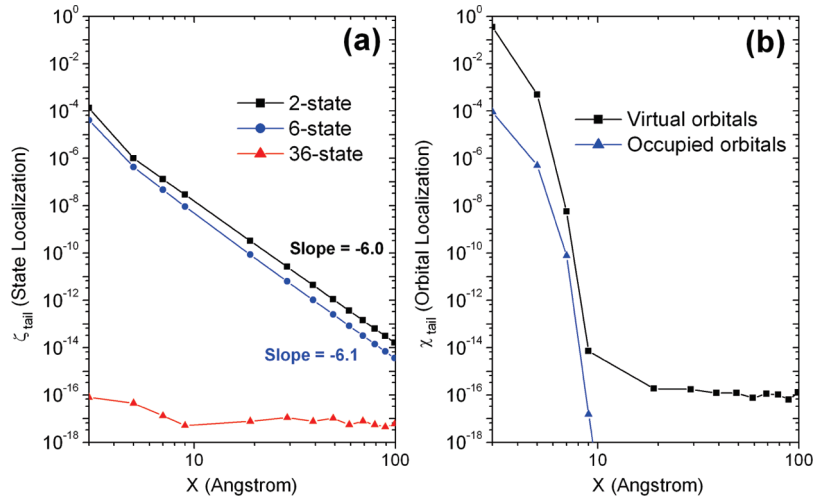

Figure 4. Quantification of the tails. (a) The ζ_{tail} function from eq 21, which quantifies the tail of the diabatic states. (b) The χ_{tail} function from eqs 24 and 25, which confirms that the localized orbitals are localized up to numerical noise at distances larger than 9 Å.

where the superscript c denotes the chopped state. This approach works only for intermolecular EET, where we can easily separate monomers. If α is far from 1, in theory the wave function should be renormalized. In our calculations, however, $|1 - \alpha| < 10^{-4}$ for $x \geq 1.5$ Å, so α is very close to 1, and we have not renormalized the diabatic states. Results using the "chopped" diabatic states are given in Figure 3. From the data, we see that the K and O terms do decay exponentially when the tail is eliminated.

4.4. Many-State Calculation. Besides chopping up the wave function, a separate and more general approach to eliminate diabatic tails is to include more than two adiabatic states in our localization scheme. As discussed in 2.3, we calculate a set of many diabatic states on the left $\{|\Xi_1^L\rangle, |\Xi_2^L\rangle, ..., |\Xi_N^L\rangle\}$ and many diabatic states on the right $\{|\Xi_1^R\rangle, |\Xi_2^R\rangle, ..., |\Xi_N^R\rangle\}$, and then we rediagonalize the Hamiltonian within each monomer subunit.

For the $(HeH)^+$ dimer, we compute these locally adiabatic diabatic states using a set of 6 or 36 adiabatic states. Note that 36 is the size of the full CIS space. From the data in Figures 3 and 4, we confirm that the tails of the diabatic states are drastically reduced if we include more states and, as expected, that the K and O terms do decay exponentially. Thus we conclude that, provided we diabatize the entire CIS subspace

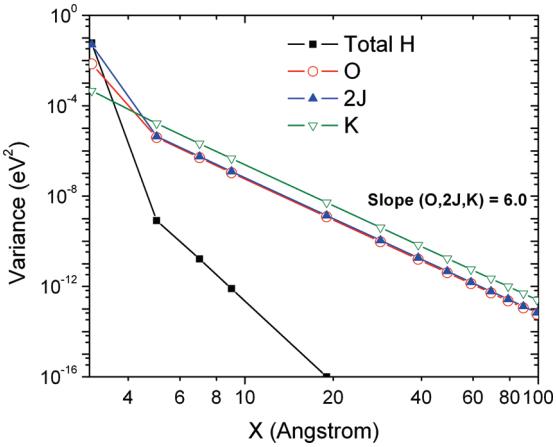

Figure 5. Variances of *J*, *K*, *O*, and *H* terms as a function of monomer separation. The variance here refers to how these values change when the number of adiabatic states is increased or the tail is chopped off directly. See eqs 28. Note that the individual components all fluctuate much more than their sum *H*.

and then rediagonlize the Hamiltonian within each monomer, we can generate diabatic states without tails.

4.5. Invariance of the Diabatic Coupling. Having shown that we can construct diabatic states with and without tails, we now must question what is the effect of these tails on the diabatic couplings. From Figure 3, one sees that the value of the *K* and *O* terms can change dramatically depending on the tails of the diabatic states. From this figure, however, one cannot clearly discern the corresponding changes in *J* and *H*. In order to highlight these changes, in Figure 5, we plot the variances. Mathematically, for each molecular geometry (specified by the distance *X*), we define the average $\bar{H}$ to be

$$\bar{H} = (H(\text{2-state}) + H(\text{6-state}) + H(\text{36-state}) + H(\text{2-state chopped}))/4 \quad (27)$$

and we compute the variance of H

$$\text{var}(H) = \frac{1}{4}[(H(\text{2-state}) - \bar{H})^2 + (H(\text{6-state}) - \bar{H})^2 + (H(\text{36-state}) - \bar{H})^2 + (H(\text{2-state chopped}) - \bar{H})^2] \quad (28)$$

The conclusion from Figure 5 is that, when we eliminate the tails of our localized diabatization, the quantities *J*, *K*, and *O* all undergo similar changes that fall off as X^{-3}, but the total value for H_{IF} changes much less than the individual components! In other words, eliminating the tails of diabatic states (either by including more states in a localized diabatization calculation or otherwise just chopping the tails off) does alter the energetic decomposition of H_{IF}, but the total diabatic coupling itself changes far less due to a cancellation of terms.

4.6. PMI-PDI Dimer. Before offering an interpretation of the data, we want to emphasize that the effects above are not small for complex systems of chemical interest. In other words, judging only from Figure 3, one might think that perhaps the discussion above was artificial because, after all, the Coulomb (*J*) term dominates the calculation of H_{IF}. Thus, is it possible that our discussion of the *K* and *O* terms is focusing on minutiae which are totally irrelevant compared to the overwhelming *J* term?

The answer is no. Although the *J* term dominates the calculation of the HeH^+ dimer, for a more complicated perylenemonoimide-perylenediimide (PMI-PDI) dimer (also considered by Hsu[52]), this is not so. To prove this point, in Figure 6, we plot the *J*, *K*, and *O* terms for the PMI-PDI dimer as a function of intermolecular distance after performing a 2-state localized diabatization, both standard (unchopped) and chopped. For the unchopped BoysOV calculation, the *O* term is comparable in size to the *J* term at long distances and is a significant contribution to *H*. When the tails are chopped, the *O* and *K* terms decay rapidly and are negligible at distances 5 Å, but the total diabatic coupling *H* is essentially unchanged from the unchopped calculation.

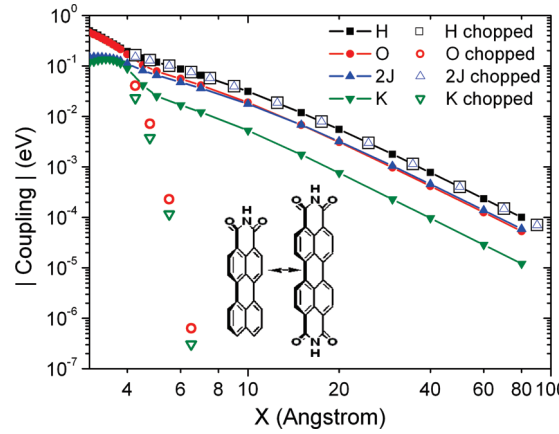

Figure 6. *J*, *K*, and *O* matrix elements that make up the total diabatic coupling *H* for the PMI-PDI dimer separated cofacially (C_s point group symmetry), using unchopped (standard) versus chopped diabatic states (respectively, filled versus empty symbols). H is calculated according to eq 20, using the relative signs of *O*, *J*, and *K* obtained for the unchopped (+,+,+) and chopped (+,−,−) results. Inset: PMI-PDI structures and stacking orientation.

This PMI-PDI calculation demonstrates that the diabatic tails in the $(HeH^+)_2$ model problem above are not atypical. Moreover, for a chemically meaningful system, this example shows that diabatic tails can lead to large redistributions of the diabatic coupling between *J*/*K*/*O* components. Thus, given the relevance of these diabatic tails for large molecules, we now want to explore their physical intepretation and the subsequent implications for modeling EET processes.

5. Theoretical Interpretation

In order to better understand the effects above, consider a dimer of model chromophores, where each chromophore has two possible excited states. We label the chromophores left (L) and right (R), and their respective excited states L*, L**, R*, and R**. We suppose that a complete basis for the electronic problem consists of four reference states $|LR^*\rangle$, $|L^*R\rangle$, $|LR^{**}\rangle$, and $|L^{**}R\rangle$. In this section, we will restrict ourselves to a Hamiltonian that is symmetric between left and right monomers. For the asymmetric case, we refer the reader to the first section of the Appendix.

Working in the basis of four states, we denote our Hamiltonian as in eq 29

$$\begin{array}{c} \\ |LR^*\rangle \\ |L^*R\rangle \\ |LR^{**}\rangle \\ |L^{**}R\rangle \end{array} \begin{array}{c} \begin{array}{cccc} |LR^*\rangle & |L^*R\rangle & |LR^{**}\rangle & |L^{**}R\rangle \end{array} \\ \begin{pmatrix} E_1^M & V & t & \gamma \\ V & E_1^M & \gamma & t \\ t & \gamma & E_2^M & W \\ \gamma & t & W & E_2^M \end{pmatrix} \end{array} \quad (29)$$

In considering the different matrix elements, we assume that the monomers are far apart so that V, W, and γ all decay as rapidly as X^{-3}, if not faster. We also assume that t is small and that, for each monomer, the second excited state is much higher in energy than the first. Altogether, we assume that $V, W, \gamma, t \ll E_2^M - E_1^M$ and we will apply perturbation theory to this problem. We also assume $V, W > 0$ without loss of generality.

5.1. Tails That Scale as X^{-3}. In order to compute the tails of diabatic states found with localized diabatization, we must diagonalize the Hamiltonian in eq 29 to find the adiabatic states. Our first step is to move to a basis of symmetric/antisymmetric states

$$|\Phi_1^{(-)}\rangle = \frac{1}{\sqrt{2}}(|\mathrm{L^*R}\rangle - |\mathrm{LR^*}\rangle)$$
$$|\Phi_1^{(+)}\rangle = \frac{1}{\sqrt{2}}(|\mathrm{L^*R}\rangle + |\mathrm{LR^*}\rangle) \quad (30)$$

$$|\Phi_2^{(-)}\rangle = \frac{1}{\sqrt{2}}(|\mathrm{L^{**}R}\rangle - |\mathrm{LR^{**}}\rangle)$$
$$|\Phi_2^{(+)}\rangle = \frac{1}{\sqrt{2}}(|\mathrm{L^{**}R}\rangle + |\mathrm{LR^{**}}\rangle) \quad (31)$$

Here, the transformed Hamiltonian is

$$\begin{array}{c} \\ |\Phi_1^{(-)}\rangle \\ |\Phi_1^{(+)}\rangle \\ |\Phi_2^{(-)}\rangle \\ |\Phi_2^{(+)}\rangle \end{array} \begin{array}{c} \begin{array}{cccc} |\Phi_1^{(-)}\rangle & |\Phi_1^{(+)}\rangle & |\Phi_2^{(-)}\rangle & |\Phi_2^{(+)}\rangle \end{array} \\ \begin{pmatrix} E_1^M - V & 0 & t-\gamma & 0 \\ 0 & E_1^M + V & 0 & t+\gamma \\ t-\gamma & 0 & E_2^M - W & 0 \\ 0 & t+\gamma & 0 & E_2^M + W \end{pmatrix} \end{array} \quad (32)$$

Next, using the zeroth order Hamiltonian H_0

$$H_0 = \begin{pmatrix} E_1^M - V & 0 & 0 & 0 \\ 0 & E_1^M + V & 0 & 0 \\ 0 & 0 & E_2^M - W & 0 \\ 0 & 0 & 0 & E_2^M + W \end{pmatrix} \quad (33)$$

the lowest two adiabatic states may be found with first order perturbation theory

$$|\Psi_1^{(-)}\rangle \approx |\Phi_1^{(-)}\rangle - \frac{t-\gamma}{E_2^M - E_1^M}|\Phi_2^{(-)}\rangle \quad (34)$$

$$|\Psi_1^{(+)}\rangle \approx |\Phi_1^{(+)}\rangle - \frac{t+\gamma}{E_2^M - E_1^M}|\Phi_2^{(+)}\rangle \quad (35)$$

The resulting diabatic states are also easily computed:

$$|\Xi_1^L\rangle = \frac{1}{\sqrt{2}}(|\Psi_1^{(+)}\rangle + |\Psi_1^{(-)}\rangle) \quad (36)$$

$$\approx |\mathrm{L^*R}\rangle - \frac{t}{E_2^M - E_1^M}|\mathrm{L^{**}R}\rangle - \frac{\gamma}{E_2^M - E_1^M}|\mathrm{LR^{**}}\rangle \quad (37)$$

$$|\Xi_1^R\rangle = \frac{1}{\sqrt{2}}(|\Psi_1^{(+)}\rangle - |\Psi_1^{(-)}\rangle) \quad (38)$$

$$\approx |\mathrm{LR^*}\rangle - \frac{t}{E_2^M - E_1^M}|\mathrm{LR^{**}}\rangle - \frac{\gamma}{E_2^M - E_1^M}|\mathrm{L^{**}R}\rangle \quad (39)$$

Although we have not shown that the adiabatic-to-diabatic transformation in eqs 36 and 38 matches the BoysOV or ER algorithms, this must be the case. After all, the symmetric case has only one possible solution according to every concievable localization algorithm.

Finally, we see that each of the diabatic states, $|\Xi_1^L\rangle$ and $|\Xi_1^R\rangle$, has some excitation on the opposite monomer. The size of this component goes as γ. For singlet electron transfer, γ will decay only as fast as the slowest component, so that $\gamma \propto X^{-3}$ according to the Coulomb coupling. Thus, we have justified why we find delocalized components in the diabatic coupling that scale as X^{-3}. As an aside, for the case of triplet EET, dealt with in refs 15, 16, 61, and 64, there is no Coulomb contribution and the tails (if any) must decay exponentially.

5.2. Stability of the H_{IF} Coupling. From the analysis above, we may now also explain why the variations in J, K, and O are significantly larger than the variations in H in Figure 5. The key point to notice is that, from eqs 29, 37, and 39

$$\langle \Xi_1^L | H | \Xi_1^R \rangle = V + O(\varepsilon^2) \quad (40)$$

Here, we denote ε as the order of our perturbation, i.e., ε is proportional to t, γ, V, and W.

The take home message from eq 40 is that, in the original basis of diabatic states, there is no first order correction to the diabatic coupling caused by the higher state. In other words, the higher excited state will contribute to the diabatic coupling only at second order, and the diabatic tails contribute only very weakly to the total diabatic coupling. However, if we decompose the diabatic coupling, we will find first order corrections to each of the J, K, and O components- but these components will all nearly cancel out in the end.

6. Discussion and Conclusion

We have presented above two different methods for EET calculations of well-separated donor−acceptor pairs. First, we computed diabatic states by rotating together only two adiabatic states. In this case, we found that electronic excitation could not be totally localized on one monomer. Moreover, we showed that, if the dimer separation is X, the amplitudes of these tails scale as X^{-3} for singlet EET.

Second, we constructed diabatic states without tails either (i) by explicitly chopping them off or (ii) by including more than two adiabatic states in our original quantum chemistry calculation, localizing all adiabatic states, and then diagonalizing the Hamiltonian within each monomer. In either case, we found

diabatic states without tails and with total diabatic coupling nearly identical to each other and to the original (2-state) approach.

Our theoretical analysis in the last section has given a partial explanation of the above phenomena. In particular, we found that diabatic tails arise mathematically because of interactions between relevant low-energy states and other high-energy states that are energetically inaccessible. At the same time, however, these tails do not contribute meaningfully to the total diabatic coupling between monomers because of a cancellation of terms; in the end, they lead only to differences in the individual components of the diabatic coupling. This explains why the diabatic coupling is nearly constant even as we include more adiabatic states and reduce the tails to zero.

Unfortunately, while all of the above statements are true, we are still lacking a clear physical interpretation of the tail phenomenon. The simplest question to ask regarding the delocalized tails of diabatic states is: Are these tails physically realistic?

On the one hand, one can argue that these tails are real, and they are effectively wrapping in information from higher excited states. In this interpretation when one monomer is electronically excited, this initial excitation forces a very small simultaneous excitation on the second monomer. In other words, when the electrons on one monomer are excited, this induces a small mean-field response from electrons on the second monomer. These excitations are small and do not lead to changes in the final diabatic coupling element, but they do represent a physical relaxation: from the adiabatic perspective, electronic excitations will always want to delocalize to some degree. Thus far, our analysis has focused exclusively on the long-range asymptotic behavior of the diabatic coupling between well-separated monomers. At short distances, these diabatic tails will be more physically significant and localized diabatization will certainly give different diabatic couplings compared to traditional methods based on isolated fragments.[15,16]

On the other hand, one can argue that these tails are only a mirage and a side-effect of starting with adiabatic states and using the 2-state approximation. In this interpretation, the correct diabatic state should have all excitation completely localized on one monomer, and delocalization with other monomers up to 99 Å away is a methodological artifact. Given that the tails are irrelevant for the final diabatic coupling (which is the key observable quantity), the tails must be an illusion. This would seem to be a strong argument for constructing diabatic states by constraining electronic excitation to one monomer, in a similar spirit to constrained DFT[46−49] or using models based on excitations calculated for isolated monomers.[63]

Ultimately, without more information, we cannot identify the correct interpretation above. After all, we have constructed diabatic states for isolated molecular systems to approximate the initial and final states of EET processes in solution. In order to discriminate between the two viewpoints described above, in the broad context of condensed phase chemistry, we would need to know about the environment interacting with the monomers. This environment perturbs the electronic structure of the isolated molecules and affects the relaxation of the excited chromophores and the nature of the excited diabatic states. To that end, we are now addressing the role of solvent in EET processes (informative analysis and computation on this topic have been reported in ref 18 and 63). Future theoretical progress should be possible in this research area if one applies a numerically tractable model interaction for the system-bath interactions: does one find a small tail of electronic excitation? More generally, what is the effect of solvent on this tail? What are the implications for EET through bridge molecules? These are critical questions now arising at the intersection between quantum chemistry and quantum dynamics.

Acknowledgment. The authors thank Mark A. Ratner for many helpful discussions and his ongoing guidance and support. We also thank Alex Sodt and Yihan Shao for computational help. This work was supported as part of the ANSER Center, an Energy Frontier Research Center funded by the U.S. Department of Energy, Office of Science, Office of Basic Energy Sciences, under Award No. DE-SC0001059. The Division of Chemical Sciences, Geosciences, and Biosciences, Office of Basic Energy Sciences of the U.S. Department of Energy is gratefully acknowledged for funding the research carried out by M.D.N. through Grant DE-AC02-98CH10886. J.E.S. was supported by Prof. Ratner through grants from the Chemistry division of the NSF and ONR, and from start-up funds at the University of Pennsylvania.

Appendix

Nonsymmetric Case. We now extend the formalism above in section 5 to the nonsymmetric dimer case to show (i) that there are tails that scale as X^{-3}, but also that (ii) for very large X these tails do not affect the overall diabatic coupling, only the J, K, and O components. However, for claim (ii), we offer only a partial proof, showing under what conditions the tails will not affect the diabatic coupling. As a practical matter, for all examples so far, we have always found that this conclusion is true: the diabatic tails barely affect the total diabatic doupling.

Working in the basis of four states, we denote our Hamiltonian as in eq 41

$$\begin{array}{c} \\ |LR^*\rangle \\ |L^*R\rangle \\ |LR^{**}\rangle \\ |L^{**}R\rangle \end{array} \begin{array}{c} \begin{array}{cccc} |LR^*\rangle & |L^*R\rangle & |LR^{**}\rangle & |L^{**}R\rangle \end{array} \\ \begin{pmatrix} E_1^L & V & t & \gamma \\ V & E_1^R & \gamma' & t' \\ t & \gamma' & E_2^L & W \\ \gamma & t' & W & E_2^R \end{pmatrix} \end{array} \tag{41}$$

As before, we will assume that V, W, γ, $\gamma' \ll t,t' \ll E_2^{\mathrm{L}} - E_1^{\mathrm{L}}$, $E_2^{\mathrm{R}} - E_1^{\mathrm{R}}$, $E_2^{\mathrm{L}} - E_1^{\mathrm{R}}$, and $E_2^{\mathrm{R}} - E_1^{\mathrm{L}}$. Note that we now enforce the fact that t, t' are not the smallest parameters (see section 5), which is reasonable given the overlap between |LR*⟩ and |LR**⟩. Again, we assume V, $W > 0$ without loss of generality.

Preliminary Transformations. In order to compute the tails of diabatic states, our first step is to diagonalize the Hamiltonian on the left and right monomers. This introduces locally adiabatic states and mixing angles θ_{L} and θ_{R}

$$\begin{pmatrix} \Phi_1^{\mathrm{L}} \\ \Phi_2^{\mathrm{L}} \end{pmatrix} = \begin{pmatrix} \cos(\theta_{\mathrm{L}}) & -\sin(\theta_{\mathrm{L}}) \\ \sin(\theta_{\mathrm{L}}) & \cos(\theta_{\mathrm{L}}) \end{pmatrix} \begin{pmatrix} \mathrm{L^*R} \\ \mathrm{L^{**}R} \end{pmatrix} \tag{42}$$

$$\begin{pmatrix} \Phi_1^{\mathrm{R}} \\ \Phi_2^{\mathrm{R}} \end{pmatrix} = \begin{pmatrix} \cos(\theta_{\mathrm{R}}) & -\sin(\theta_{\mathrm{R}}) \\ \sin(\theta_{\mathrm{R}}) & \cos(\theta_{\mathrm{R}}) \end{pmatrix} \begin{pmatrix} \mathrm{LR^*} \\ \mathrm{LR^{**}} \end{pmatrix} \tag{43}$$

The transformed Hamiltonian is

$$\begin{array}{c} \\ |\Phi_1^L\rangle \\ |\Phi_1^R\rangle \\ |\Phi_2^L\rangle \\ |\Phi_2^R\rangle \end{array} \begin{array}{c} \begin{array}{cccc} |\Phi_1^L\rangle & |\Phi_1^R\rangle & |\Phi_2^L\rangle & |\Phi_2^R\rangle \end{array} \\ \begin{pmatrix} \tilde{E}_1^L & \tilde{V} & 0 & \tilde{\gamma} \\ \tilde{V} & \tilde{E}_1^R & \tilde{\gamma}' & 0 \\ 0 & \tilde{\gamma}' & \tilde{E}_2^L & \tilde{W} \\ \tilde{\gamma} & 0 & \tilde{W} & \tilde{E}_2^R \end{pmatrix} \end{array} \tag{44}$$

Note that, to first order, $\cos(\theta_{\mathrm{L}}) = \cos(\theta_{\mathrm{R}}) \approx 1$ and $\tilde{V} \approx V$.

Next, we diagonalize the Hamiltonian in the subspace of the two lowest lying states, which leads to another mixing angle, θ_1. The resulting states are

$$\begin{pmatrix} \Phi_1^{\mathrm{A}} \\ \Phi_2^{\mathrm{B}} \end{pmatrix} = \begin{pmatrix} \cos(\theta_1) & -\sin(\theta_1) \\ \sin(\theta_1) & \cos(\theta_1) \end{pmatrix} \begin{pmatrix} \Phi_1^{\mathrm{L}} \\ \Phi_1^{\mathrm{R}} \end{pmatrix} \tag{45}$$

and there is yet another transformed Hamiltonian

$$\begin{array}{c} \\ |\Phi_1^A\rangle \\ |\Phi_1^B\rangle \\ |\Phi_2^L\rangle \\ |\Phi_2^R\rangle \end{array} \begin{array}{c} \begin{array}{cccc} |\Phi_1^A\rangle & |\Phi_1^B\rangle & |\Phi_2^L\rangle & |\Phi_2^R\rangle \end{array} \\ \begin{pmatrix} E_1^A & 0 & \varepsilon_{AL} & \varepsilon_{AR} \\ 0 & E_1^B & \varepsilon_{BL} & \varepsilon_{BR} \\ \varepsilon_{AL} & \varepsilon_{BL} & \tilde{E}_2^L & \tilde{W} \\ \varepsilon_{AR} & \varepsilon_{BR} & \tilde{W} & \tilde{E}_2^R \end{pmatrix} \end{array} \tag{46}$$

At this point, all of the quantities ε_{ij} are perturbations. Applying perturbation theory to first-order, with zeroth-order Hamiltonian H_0

$$H_0 = \begin{pmatrix} E_1^{\mathrm{A}} & 0 & 0 & 0 \\ 0 & E_1^{\mathrm{B}} & 0 & 0 \\ 0 & 0 & \tilde{\mathrm{E}}_2^{\mathrm{L}} & 0 \\ 0 & 0 & 0 & \tilde{\mathrm{E}}_2^{\mathrm{R}} \end{pmatrix} \tag{47}$$

we conclude that the two lowest eigenstates (or adiabatic states) of the system are

$$|\Psi_1^{\mathrm{A}}\rangle \approx |\Phi_1^{\mathrm{A}}\rangle + \frac{\varepsilon_{\mathrm{AL}}}{E_1^{\mathrm{A}} - \tilde{\mathrm{E}}_2^{\mathrm{L}}}|\Phi_2^{\mathrm{L}}\rangle + \frac{\varepsilon_{\mathrm{AR}}}{E_1^{\mathrm{A}} - \tilde{\mathrm{E}}_2^{\mathrm{R}}}|\Phi_2^{\mathrm{R}}\rangle + ... \tag{48}$$

$$|\Psi_1^{\mathrm{B}}\rangle \approx |\Phi_1^{\mathrm{B}}\rangle + \frac{\varepsilon_{\mathrm{BL}}}{E_1^{\mathrm{B}} - \tilde{\mathrm{E}}_2^{\mathrm{L}}}|\Phi_2^{\mathrm{L}}\rangle + \frac{\varepsilon_{\mathrm{BR}}}{E_1^{\mathrm{B}} - \tilde{\mathrm{E}}_2^{\mathrm{R}}}|\Phi_2^{\mathrm{R}}\rangle + ... \tag{49}$$

Tails That Scale as X^{-3}. The states $|\Psi_1^{\mathrm{A}}\rangle$ and $|\Psi_1^{\mathrm{B}}\rangle$ are are the lowest-lying adiabatic states that we calculate in CIS calculations. In order to transform these states back into diabatic states, $|\Xi_1^{\mathrm{L}}\rangle$ and $|\Xi_1^{\mathrm{R}}\rangle$, we need an adiabatic-to-diabatic transformation matrix (with an implied mixing angle θ_{F})

$$\begin{pmatrix} \Xi_1^{\mathrm{L}} \\ \Xi_1^{\mathrm{R}} \end{pmatrix} = \begin{pmatrix} \cos(\theta_{\mathrm{F}}) & -\sin(\theta_{\mathrm{F}}) \\ \sin(\theta_{\mathrm{F}}) & \cos(\theta_{\mathrm{F}}) \end{pmatrix} \begin{pmatrix} \Psi_1^{\mathrm{A}} \\ \Psi_1^{\mathrm{B}} \end{pmatrix} \tag{50}$$

From the form of eqs 48 and 49, however, it is clear that, in general, we can no longer rotate adiabatic states into diabatic states with all electronic excitation localized purely on one monomer. Instead, we find that, for a molecule with electronic excitation on the left monomer, there is a tail of excitation on the right monomer. More precisely, we expect that the form of the diabatic states will be

$$|\Xi_1^{\mathrm{L}}\rangle = |\Phi_1^{\mathrm{L}}\rangle + c_{\mathrm{LL}}|\Phi_2^{\mathrm{L}}\rangle + c_{\mathrm{LR}}|\Phi_2^{\mathrm{R}}\rangle + ... \tag{51}$$

$$|\Xi_1^{\mathrm{R}}\rangle = |\Phi_1^{\mathrm{R}}\rangle + c_{\mathrm{RL}}|\Phi_2^{\mathrm{L}}\rangle + c_{\mathrm{RR}}|\Phi_2^{\mathrm{R}}\rangle + ... \tag{52}$$

where c_{ij} is of the same order of magniutude as ε_{ij}, both scaling as X^{-3}. Thus, the function ζ_{tail} in eq 21 must scale as X^{-6}.

Stability of the H_{IF} Coupling. To show that the diabatic coupling is largely unperturbed by the diabatic tails, note that

$$\begin{pmatrix} \langle\Psi_1^{\mathrm{A}}|H|\Psi_1^{\mathrm{A}}\rangle & \langle\Psi_1^{\mathrm{A}}|H|\Psi_1^{\mathrm{B}}\rangle \\ \langle\Psi_1^{\mathrm{B}}|H|\Psi_1^{\mathrm{A}}\rangle & \langle\Psi_1^{\mathrm{B}}|H|\Psi_1^{\mathrm{B}}\rangle \end{pmatrix} = \begin{pmatrix} \langle\Phi_1^{\mathrm{A}}|H|\Phi_1^{\mathrm{A}}\rangle & \langle\Phi_1^{\mathrm{A}}|H|\Phi_1^{\mathrm{B}}\rangle \\ \langle\Phi_1^{\mathrm{B}}|H|\Phi_1^{\mathrm{A}}\rangle & \langle\Phi_1^{\mathrm{B}}|H|\Phi_1^{\mathrm{B}}\rangle \end{pmatrix} + O(\varepsilon^2) \tag{53}$$

This equivalence to first order follows from perturbation theory and is applicable only to the H matrix element, not to the individual J, K, and O contributions. Note that by construction the off-diagonal elements on the right-hand side are zero to first order in eq 53.

Suppose now that the final adiabatic-to-diabatic rotation is exactly the inverse of the earlier transformation from locally adiabatic states to diabatic states, i.e., $\theta_{\mathrm{F}} = -\theta_1$ in eqs 45 and 50. If this is true, then both the adiabatic Hamiltonian and the adiabatic-to-diabatic mixing angles are identical to first order for two different scenarios:

- We compute only two adiabatic states.
- We compute many adiabatic states and, from these, we generate diabatic states that are completely localized without tails.

It follows therefore that the final diabatic coupling must also be unchanged for these two different scenarios, with $H_{\mathrm{IF}} \approx \tilde{V} \approx V$ (see eq 44). Thus, we have shown that the diabatic tails should not affect the total diabatic coupling, provided we make the ad hoc assumption that the mixing angle for the first order states be identical to the mixing angle for the zeroth order states, $\theta_{\mathrm{F}} = -\theta_1$. Although this approximation need not be true, it is exact for symmetric dimers, where $\theta_{\mathrm{F}} = -\theta_1 = \pi/4$. For the more general asymmetric case, we have been unable to prove this assertion mathematically. As noted in the paper, however, we do find empirically that the final diabatic coupling is nearly unchanged as a result of the diabatic tail.

Comparison Between Our Diabatic Couplings and Those of Hsu and Co-workers. We mentioned in 3.1 that the coupling in eq 20 is not the same as that predicted by Hsu and co-workers.[51,63,67] We demonstrate this now explicitly. According to Hsu and co-workers, the diabatic coupling for EET evolves from three terms, $J = J_{\mathrm{Coulomb}} + J_{\mathrm{Exch}} + J_{\mathrm{Overlap}}$, each defined in terms of transition densities (using Hsu's notation and sign convention)[67]

$$J_{\mathrm{Coulomb}} = \int \mathrm{d}r \int \mathrm{d}r' \, \rho_{\mathrm{D}}{}^*(r, r) \frac{1}{|r - r'|} \rho_{\mathrm{A}}(r', r') \tag{54}$$

$$J_{\text{Exchange}} = \int \mathrm{d}r \int \mathrm{d}r' \, \rho_{\text{D}}^*(r,r') \frac{1}{|r-r'|} \rho_{\text{A}}(r',r) \tag{55}$$

$$J_{\text{Overlap}} = -\int \mathrm{d}r \, \rho_{\text{D}}^*(r,r) \rho_{\text{A}}(r,r) \omega_0 \tag{56}$$

$$\rho_{\text{D}}(r,r') \equiv N \int \mathrm{d}r_2 \, \mathrm{d}r_3 \ldots \mathrm{d}r_N \, \Psi_{\text{DA}}(r,r_2,r_3,\ldots,r_N) \Psi_{\text{D*A}}^*(r',r_2,r_3,\ldots,r_N) \tag{57}$$

$$\rho_{\text{A}}(r,r') \equiv N \int \mathrm{d}r_2 \, \mathrm{d}r_3 \ldots dr_N \Psi_{DA}(r,r_2,r_3,\ldots,r_N) \Psi_{DA^*}^*(r',r_2,r_3,\ldots,r_N) \tag{58}$$

where ω_0 is the frequency of the transition, N is the number of electrons, and the spin degrees of freedom have been integrated out. Because the overlap term evolves from the nonorthogonality of donor and acceptor fragments, we will ignore this term when comparing to our approach which uses orthonormal diabatic states.

In the language of the present paper, we will define D*A as the initial state I and DA* as the final state F. We will work with a HF ground state, so that $|\Psi_{\text{DA}}\rangle = |\Psi_{\text{HF}}\rangle$. Thus, if the singlet diabatic states are defined by

$$|\Psi_{\text{I}}\rangle = \sum_{ia} \frac{t_i^{\text{I}a}}{\sqrt{2}} (|\Phi_i^a\rangle + |\Phi_{\bar{i}}^{\bar{a}}\rangle) = \sum_{ia} \frac{t_i^{\text{I}a}}{\sqrt{2}} (c_a^\dagger c_i + c_{\bar{a}}^\dagger c_{\bar{i}}) |\Phi_{\text{HF}}\rangle \tag{59}$$

$$|\Psi_{\text{F}}\rangle = \sum_{ia} \frac{t_i^{\text{F}a}}{\sqrt{2}} (|\Phi_i^a\rangle + |\Phi_{\bar{i}}^{\bar{a}}\rangle) = \sum_{ia} \frac{t_i^{\text{F}a}}{\sqrt{2}} (c_a^\dagger c_i + c_{\bar{a}}^\dagger c_{\bar{i}}) |\Phi_{\text{HF}}\rangle \tag{60}$$

then we can calculate transition densities according to

$$\rho_{\text{D}}(r,r') = \langle \Psi_{\text{HF}} | c_r^\dagger c_{r'} | \Psi_{\text{F}} \rangle = \sqrt{2} \sum_{ia} t_i^{\text{F}a} \phi_i(r) \phi_a(r') \tag{61}$$

$$\rho_{\text{A}}(r,r') = \langle \Psi_{\text{HF}} | c_r^\dagger c_{r'} | \Psi_{\text{I}} \rangle = \sqrt{2} \sum_{ia} t_i^{\text{I}a} \phi_i(r) \phi_a(r') \tag{62}$$

Here $\phi_i(r)$ and $\phi_j(r)$ are occupied spatial molecular orbitals and $\phi_a(r)$ and $\phi_b(r)$ are virtual spatial molecular orbitals. We assume that all such orbitals are real and once again all spin degrees of freedom have been integrated out. We have also used the convenient relationship $c_p^\dagger = \sum_r \phi_p(r) c_r^\dagger$ and $c_r^\dagger = \sum_p \phi_p(r) c_r^\dagger$; this assumes in principle a complete atomic orbital basis so that we may convert between molecular orbitals and the position "r" basis.

Using eqs 54, 55, 61, and 62, it follows that

$$J_{\text{Coulomb}} = 2 \sum_{ia\,jb} t_i^{\text{I}a} t_j^{\text{F}b} (ia|jb) \tag{63}$$

$$J_{\text{Exchange}} = 2 \sum_{ia\,jb} t_i^{\text{I}a} t_j^{\text{F}b} (ij|ab) \tag{64}$$

Comparing to section 3.1, we see that the exchange coupling as calculated by Hsu and co-workers does not match the exchange term in eq 20. In particular, we find that there is an extra factor of 2 in eq 64 and a change of sign. Note, however, that the Hsu approach matches our results much better if one uses a spin-dependent transition density, e.g. $\rho_{\text{D}}(\sigma r,\sigma r')$, with an additional sign change for J_{Exchange}.

Lastly, we observe that our "one-electron" term is distinctly different from their "overlap" term. For example, eq 20 includes the Fock operator, which contains a kinetic energy component, while eq 56 does not.

References and Notes

(1) Koppel, H. In *Conical Intersections: Electronic Structure, Dynamics and Spectroscopy*; Domcke, W., Yarkony, D. R., Koppel, H., Eds.; World Scientific Publishing Co.: Hackensack, NJ, 2004; p 175.

(2) Cederbaum, L. S. In *Conical Intersections: Electronic Structure, Dynamics and Spectroscopy*; Domcke, W., Yarkony, D. R., Koppel, H., Eds.; World Scientific Publishing Co.: Hackensack, NJ, 2004; p 3.

(3) Baer, M. *Beyond Born-Oppenheimer: Electronic Nonadiabatic Coupling Terms and Conical Intersections*; Wiley: New York, 2006.

(4) Van Voorhis, T.; Kowalczyk, T.; Kaduk, B.; Wang, L. P.; Cheng, C. L.; Wu, Q. *Annu. Rev. Phys. Chem.* **2010**, *61*, 149–170.

(5) Subotnik, J. E.; Cave, R. J.; Steele, R. P.; Shenvi, N. *J. Chem. Phys.* **2009**, *130*, 234102.

(6) Subotnik, J. E.; Yeganeh, S.; Cave, R. J.; Ratner, M. A. *J. Chem. Phys.* **2008**, *129*, 244101.

(7) Turro, N. J.; Ramamurthy, V.; Scaiano, J. C. *Principles of Molecular Photochemistry*; University Science Books: Sausalito, CA, 2008.

(8) Kelley, R. F.; Tauber, M. J.; Wasielewski, M. R. *Angew. Chem., Int. Ed.* **2006**, *45*, 7979–7982.

(9) Gunderson, V. L.; Wilson, T. M.; Wasielewski, M. R. *J. Phys. Chem. C* **2009**, *113*, 11936–11942.

(10) Förster, T. *Naturwissenschaften* **1946**, *6*, 166.

(11) Jang, S.; Jung, Y.; Silbey, R. *J. Chem. Phys.* **2002**, *275*, 319.

(12) Beljonne, D.; Curutchet, C.; Scholes, G. D.; Silbey, R. J. *J. Phys. Chem. B* **2009**, *113*, 6583–6599.

(13) Dexter, D. L. *J. Chem. Phys.* **1953**, *21*, 836.

(14) Nitzan, A. *Chemical Dyanmics in Condensed Phases*; Oxford University Press: New York, 2006.

(15) Scholes, G. D.; Harcourt, R. D.; Ghiggino, K. P. *J. Chem. Phys.* **1995**, *102*, 9574.

(16) Harcourt, R. D.; Scholes, G. D.; Ghiggino, K. P. *J. Chem. Phys.* **1994**, *101*, 10521.

(17) Craig, D. P.; Thirunamachandran, T. *Chem. Phys.* **1992**, *167*, 229–240.

(18) Iozzi, M. F.; Mennucci, B.; Tomasi, J.; Cammi, R. *J. Chem. Phys.* **2004**, *120*, 7029–7040.

(19) Yeow, E. K. L.; Haines, D. J.; Ghiggino, K. P.; Paddon-Row, M. N. *J. Phys. Chem. A* **1999**, *103*, 6517–6524.

(20) Scholes, G. D.; Ghiggino, K. P.; Oliver, A. M.; Paddon-Row, M. N. *J. Phys. Chem.* **1993**, *97*, 11871–11876.

(21) McConnell, H. M. *J. Chem. Phys.* **1961**, *35*, 508.

(22) Onuchic, J. N.; Beratan, D. N. *J. Chem. Phys.* **1990**, *92*, 722.

(23) Kurnikov, I. V.; Beratan, D. N. *J. Chem. Phys.* **1996**, *105*, 9561.

(24) Beratan, D. N.; Skourtis, S. S. *Curr. Opin. Chem. Biol.* **1998**, *2*, 235.

(25) Stuchebrukhov, A. A. *Chem. Phys. Lett.* **1994**, *225*, 55.

(26) Stuchebrukhov, A. A. *Adv. Chem. Phys.* **2001**, *118*, 1.

(27) Larsson, S.; Rodriguez-Monge, L. *J. Photochem. Photobiol. A* **1994**, *82*, 61.

(28) Hsu, C. P.; Marcus, R. A. *J. Chem. Phys.* **1997**, *106*, 584.

(29) Smith, F. T. *Phys. Rev.* **1969**, *179*, 111.

(30) O'Malley, T. F. In *Advances in Atmic and Molecular Physics*; Bates, D. R., Esterman, I., Eds.; Academic Press: New York, 1971; Vol. 7, p 223.

(31) Baer, M. *Chem. Phys. Lett.* **1975**, *35*, 112.

(32) Mead, C. A.; Truhlar, D. G. *J. Chem. Phys.* **1982**, *77*, 6090.

(33) Top, Z. H.; Baer, M. *J. Chem. Phys.* **1977**, *66*, 1363.

(34) Baer, M. *Mol. Phys.* **1980**, *40*, 1011.

(35) Pacher, T.; Cederbaum, L. S.; Koppel, H. *J. Chem. Phys.* **1988**, *89*, 7367.

(36) Pacher, T.; Cederbaum, L. S.; Koppel, H. *Adv. Chem. Phys.* **1993**, *84*, 293.

(37) Domcke, W.; Woywood, C. *Chem. Phys. Lett.* **1993**, *216*, 362.

(38) Domcke, W.; Woywood, C.; Stengle, M. *Chem. Phys. Lett.* **1994**, *226*, 257.
(39) Ruedenberg, K.; Atchity, G. J. *J. Chem. Phys.* **1993**, *99*, 3799.
(40) Atchity, G. J.; Ruedenberg, K. *Theor. Chem. Acc.* **1997**, *97*, 47.
(41) Nakamura, H.; Truhlar, D. G. *J. Chem. Phys.* **2001**, *115*, 10353.
(42) Nakamura, H.; Truhlar, D. G. *J. Chem. Phys.* **2002**, *117*, 5576.
(43) Nakamura, H.; Truhlar, D. G. *J. Chem. Phys.* **2003**, *118*, 6816.
(44) Cave, R. J.; Newton, M. D. *Chem. Phys. Lett.* **1996**, *249*, 15.
(45) Cave, R. J.; Newton, M. D. *J. Chem. Phys.* **1997**, *106*, 9213.
(46) Wu, Q.; Van Voorhis, T. *Phys. Rev. A* **2005**, *72*, 024502.
(47) Wu, Q.; Van Voorhis, T. *J. Chem. Theor. Comp.* **2006**, *2*, 765.
(48) Wu, Q.; Van Voorhis, T. *J. Phys. Chem. A* **2006**, *110*, 9212.
(49) Wu, Q.; Van Voorhis, T. *J. Chem. Phys.* **2006**, *125*, 164105.
(50) Voityuk, A. A.; Rosch, N. *J. Chem. Phys.* **2002**, *117*, 5607.
(51) Hsu, C. P.; You, Z. Q.; Chen, H. C. *J. Phys. Chem. C* **2008**, *112*, 1204.
(52) Chen, H. C.; You, Z. Q.; Hsu, C. P. *J. Chem. Phys.* **2008**, *129*, 084708.
(53) Hsu, C. P. *Acc. Chem. Res.* **2009**, *42*, 509.
(54) Edmiston, C.; Ruedenberg, K. *Rev. Mod. Phys.* **1963**, *35*, 457.
(55) Boys, S. F. *Rev. Mod. Phys.* **1960**, *32*, 296.
(56) Foster, J. M.; Boys, S. F. *Rev. Mod. Phys.* **1960**, *32*, 300.
(57) Boys, S. F. In *Quantum Theory of Atoms, Molecules and the Solid State*; Lowdin, P., Ed.; Academic Press: New York, 1966; p 253.
(58) Pipek, J.; Mezey, P. G. *J. Chem. Phys.* **1989**, *90*, 4916.
(59) Kleier, D. A.; Halgren, T. A.; Hall, J. H.; Lipscomb, W. N. *J. Chem. Phys.* **1974**, *61*, 3905.
(60) Subotnik, J. E.; Shao, Y.; Liang, W.; Head-Gordon, M. *J. Chem. Phys.* **2004**, *121*, 9220.
(61) Subotnik, J. E.; Vura-Weis, J.; Sodt, A.; Ratner, M. A. *J. Phys. Chem. A* **2010**, 10.1021/jp101235a.
(62) David Sherrill CIS notes: http://vergil.chemistry.gatech.edu/notes/cis/cis.html.
(63) Hsu, C. P.; Fleming, G.; Head-Gordon, M.; Head-Gordon, T. *J. Chem. Phys.* **2001**, *114*, 3065.
(64) Krueger, B. P.; Scholes, G. D.; Fleming, G. R. *J. Phys. Chem. B* **1998**, *102*, 9603–9604.
(65) Shao, Y.; et al. *Phys. Chem. Chem. Phys.* **2006**, *8*, 3172–3191.
(66) Head-Gordon, M.; Grana, A. M.; Maurice, D.; White, C. A. *J. Phys. Chem.* **1995**, *99*, 14261.
(67) You, Z.-Q.; Hsu, C.-P. *J. Chem. Phys.* **2010**, *133*, 074105.

JP104783R